Accepted Manuscript

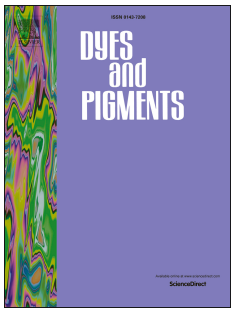

Development of a two-photon carbazole derivative probe for fluorescent visualization of G-quadruplex DNA in cells

Fengli Gao, Shuhua Cao, Wen Sun, Saran Long, Jiangli Fan, Xiaojun Peng

PII: S0143-7208(19)31202-1

DOI: https://doi.org/10.1016/j.dyepig.2019.107749

Article Number: 107749

Reference: DYPI 107749

To appear in: *Dyes and Pigments*

Received Date: 24 May 2019

Revised Date: 23 July 2019

Accepted Date: 23 July 2019

Please cite this article as: Gao F, Cao S, Sun W, Long S, Fan J, Peng X, Development of a two-photon carbazole derivative probe for fluorescent visualization of G-quadruplex DNA in cells, *Dyes and Pigments* (2019), doi: https://doi.org/10.1016/j.dyepig.2019.107749.

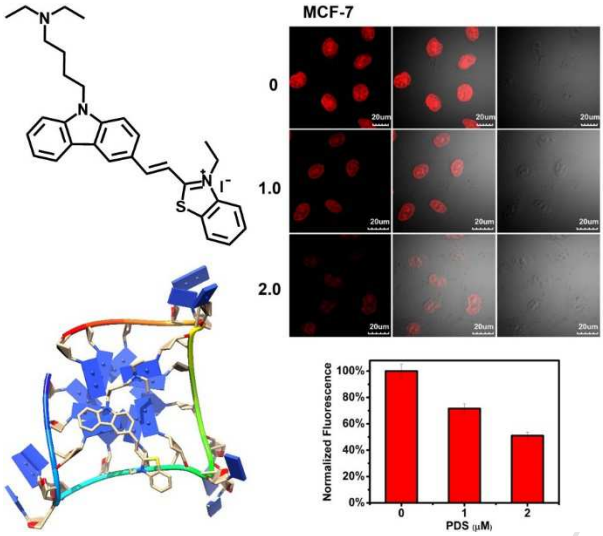

The molecule structure and docking calculation with G4 DNA of two-photon carbazole based fluorescent probe (**CZ-BT**) which is specific on G4 DNA in cells.

Development of a two-photon carbazole derivative probe for fluorescent visualization of G-quadruplex DNA in cells

Fengli Gao,‡[a] Shuhua Cao,‡[b] Wen Sun,[ac] Saran Long,*[ac] Jiangli Fan,*[ac] and Xiaojun Peng,[ac]

a. State Key Laboratory of Fine Chemicals, Dalian University of Technology, 2 Linggong Road, High-Tech district, Dalian 116024, China

b. College of chemistry, chemical and environmental engineering, Weifang University, No. 5147 Dongfeng Street, Weifang, 261061, China.

c. Shenzhen Research Institute, Dalian University of Technology, Nanshan District, Shenzhen, 518057, P.R. China.

E-mail: fanjl@dlut.edu.cn, srlong@dlut.edu.cn

‡ These authors contributed equally to this work.

Abstract: G-quadruplex (G4) sequences are considered to play important roles in gene regulation, therefore the development of selective and sensitive probes for G4 DNAs is important for studying the functions of G-rich gene sequences, as well as designing of novel and effective anticancer drugs. Herein, a carbazole derivative (**CZ-BT**) was synthesized and characterized by a simple process for G4 DNA detection. **CZ-BT** was preferentially bound with G4 DNA compared with other types of nucleic acids according to the fluorescence assays. The fluorescence intensity and fluorescence lifetime of **CZ-BT** significantly increased after the interaction with G4 DNA. Molecular docking calculation proved the π-π stacking binding mode between **CZ-BT** and G4 DNA. Furthermore, the specificity of **CZ-BT** on G4 DNA was well demonstrated with the contrast of pyridostatin (PDS, a classical G-quadruplex ligand) using two-photon confocal fluorescent imaging technique and cell cycle experiment in cells. We believe that this study would give some favorable factors on developing of highly effective fluorescent probes for G4 DNA applications.

Keywords: two-photon; carbazole derivative; fluorescent probe; G-quadruplex DNA; pyridostatin

1. Introduction

G-quadruplex DNAs (G4 DNAs) are noncanonical secondary DNA structures formed by self-assembly of guanine rich nucleic acid sequences at the conditions of specific ionic strength and pH values [1-2]. Owing to the direction of strands or parts of a strand that form

the tetrads, the structures of G4 DNAs are displayed as parallel, antiparallel, and mixed types [3]. Researches reveal that G4 DNAs distribute in the regions which are closely related to the gene functions, such as telomere and promoter regions [4-6]. They play an important role in maintaining the stability of chromosome and are closely related to cancer initiation and progression [7-11]. Therefore, it is of great biological significance for tracking and detecting of G4 DNAs.

Up to now, several analytical tools are employed for the research of G4 DNAs, such as electrochemistry [12-14], monoclonal antibodies [7,15], fluorescent probes [16-19], and so on. Electrochemistry method is beneficial to miniaturization in terms of the instrumentation, while the instable electrochemical signals lead to poor reproducibility. Monoclonal antibodies have been implemented for G4 DNAs detection by means of secondary, labelled antibodies. However, a number of issues were raised, including artefacts caused by chromatin fixation and induced G4 formation [20]. In recent years, although some fluorescent small probes for G4 DNAs have been developed due to their advantages of high sensitivity and low cost, some of them with the short emission wavelength, poor selectivity and lack of relevant cell experiments restricted their further applications [21-23].

Due to the excitation source of long wavelength (>700 nm), the two-photon microscopy can effectively avoid the interference of autofluorescence and has widely been used for imaging cells and tissues [24-26]. While the correlative research of two-photon fluorescent probes on G4 DNAs are less [27-28]. Herein, with excellent optical properties, a novel two-photon carbazole derivative probe (**CZ-BT**) for G4 DNA was designed and synthesized (Scheme 1). In this probe, the conjugated complex of carbazole-benzothiazole possessed an extended delocalized π-electron system which could interact with G4 DNA by π-π stacking. The diethyl amine group was introduced to increase the hydrophilic and positive charged benzothiazole was more easily to contact with DNA. Molecular docking calculation validated the π-π stacking binding mode between **CZ-BT** and G4 DNA. The two-photon confocal fluorescent images and cell cycle experiment of **CZ-BT** and PDS fully proved the specificity on G4 DNA.

2. Experimental section

2.1. Reagents and materials

Ultrapure water used in the whole experiment was from Milli-Q systems, other reagents and solvents were of analytical grade without further purification. Tris-HCl (10 mM, pH=7.4, 60 mM KCl) buffer solution was used for the whole solution test. Silica column chromatography was performed using silica gel (200-300 mesh, Qingdao Ocean Chemicals). The G-quadruplet binding ligand pyridostatin (PDS) was purchased from Sigma-Aldrich. Hoechst 33342, DNase and RNase were purchased from Thermo Fisher Scientific. MCF-7 and COS7 cells were obtained from Shanghai Sangon Biotechnology Co., Ltd. (Shanghai, China). The absolute fluorescent quantum yields of **CZ-BT** in various conditions were recorded by Quanturus-QY (Hamamatsu C11347-11, Japan). MCF-7 and COS7 cells fluorescent images were recorded on confocal laser fluorescent scanning microscope (Olympus, FV1000, Japan). Cell cycle experiment was recorded on Acoustic focusing cytometer of Thermo Fisher Scientific (Attune NxT).

2.2 DNA synthesis and purification

Table 1. Sequences of oligonucleotides used in the present study.

Name	Sequence	Structure
dA21	5`-d(AAAAAAAAAAAAAAAAAAAAA)-3`	Single stranded
dT21	5`-d(TTTTTTTTTTTTTTTTTTTTT)-3`	Single stranded
ss26	5`-d(ATACGATGCTTCACGGTGCTATCTG)-3`	Single stranded
ssDNA	5`-d(GGATGTGAGTGTGAGTGTGAGG)-3`	Single stranded
Poly(A-T)$_9$	5`-d(ATATATATATATATATAT)-3`	Duplex
Poly(G-C)$_9$	5`-d(GCGCGCGCGCGCGCGCGC)-3`	Duplex
Hum24	5`-(TTAGGGTTAGGGTTAGGGTTAGGG)-3`	G4 DNA
Telo21	5`-d(GGGTTAGGGTTAGGGTTAGGG)-3`	G4 DNA
Oxy12	5`-d(GGGGTTTTGGGG)-3`	G4 DNA
Pu22	5`-d(TGAGGGTGGGTAGGGTGGGTAA)-3`	G4 DNA

All oligonucleotides used in this work were synthesized and HPLC purified by TaKaRa Biotechnology Co., Ltd. (Dalian, China), and the sequences were listed in Table 1. The original DNA sequences were dissolved in TE buffer and stored at -20°C for further use. To

obtain DNA formation information, oligonucleotides were pre-treated in Tris-HCl buffer (10 mM, pH=7.4, containing 60 mM KCl) by raising the temperature to 95°C and keeping for 5 min, and then gradually cooling down to room temperature.

*2.3. Synthetic procedures of **CZ-BT***

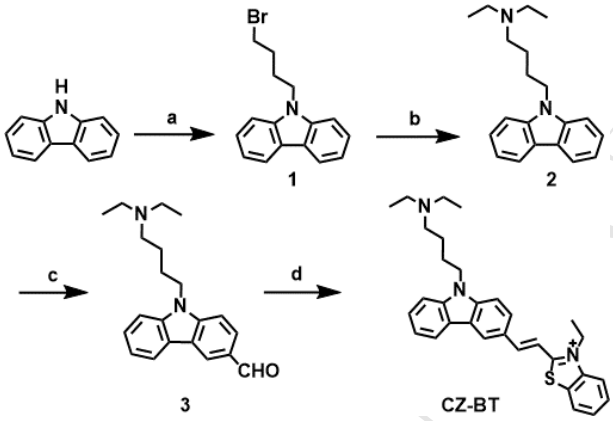

Scheme 1. Synthesis route of the G4 DNA probe **CZ-BT**: (a) acetone, KOH, rt, 24 h, 80%; (b) THF, Na_2CO_3, N_2, reflux, 24 h, 65%; (c) DMF, $POCl_3$, 100, 4 h, 43%; (d) ethanol, piperidine, N_2, reflux, 10 h, 24%.

9-(4-bromobutyl)-9H-carbazole (1)

To a solution of carbazole (499 mg, 3 mmol) in 20 mL of acetone, 0.33 mL of 1,4-dibromobutane (3 mmol, 603 mg) and a catalytic amount of KOH were added. After stirring for 24 hours at room temperature, the solvent was removed under reduced pressure. Then the residue was purified by silica gel column chromatography (petroleum ether: dichloromethane = 4:1, v/v) to afford the final compound of white solid (725 mg, 80%). ^{1}H NMR (400 MHz, $CDCl_3$) δ 8.10 (s, 1H), 7.43 (dd, J = 24.4, 6.6 Hz, 2H), 4.34 (d, J = 5.7 Hz, 1H), 3.36 (d, J = 5.3 Hz, 1H), 2.24 – 1.78 (m, 2H); TOF HRMS: m/z calcd for $C_{16}H_{16}NBr^+$ M^+: 303.0549, found: 304.0552.

N, N-Diethyl-9H-carbazole-9-butanamine (2)

A reaction mixture which containing 9-(bromobutyl)-9H-carbazole (3.02g, 10 mmol), diethylamine (1.0 mL, 10mmol) and a catalytic amount of Na_2CO_3 in tetrahydrofuran (20 mL) was refluxed for 24 hours within the protection of nitrogen. After cooling down to room

temperature, the mixture was filtered, and the filtrate was extracted with ethyl acetate, dried over Na_2SO_4, concentrated. The residue was purified with a silica gel column and was eluted with dichloromethane and CH_3OH (50:1, v/v) to afford 1.91 g (65%) of the compound. ^{1}H NMR (400 MHz, MeOD) δ 8.07 (d, J = 7.8 Hz, 1H), 7.46 (dt, J = 14.5, 7.8 Hz, 2H), 7.18 (t, J = 7.4 Hz, 1H), 4.42 (t, J = 6.9 Hz, 1H), 2.56 – 2.35 (m, 3H), 1.96 – 1.80 (m, 1H), 1.61 – 1.42 (m, 1H), 0.95 (t, J = 7.2 Hz, 3H). TOF HRMS: m/z calculated for $C_{20}H_{26}N_2^+$ M^+: 294.2155, found: 295.2161.

9-(4-(diethylamino) butyl)-9H-carbazole-3-carbaldehyde (3)

To a solution of N, N-Diethyl-9H-carbazole-9-butanamine (1.61 g, 5 mmol) in DMF (5 mL), $POCl_3$ (0.9 mL, 20 mmol) was added into the solution in ice-water bath under the protection of nitrogen. The mixture was stirred vigorously for half an hour, then the temperature was risen to 100°C and continued for 4 hours. The nigger-brown reaction mixture was poured into a solution of sodium acetate (20% mass fraction) to neutralize the acidity and then extracted with ethyl acetate. The solvent was dried with anhydrous sodium sulfate overnight and evaporated on a rotary evaporation. The crude product was purified on a silica gel column using dichloromethane and CH_3OH (40:1, v/v) as eluent, yielding 693 mg (43%) of the desired product as light yellow power. ^{1}H NMR (400 MHz, MeOD) δ 10.00 (s, 1H), 8.63 (d, J = 1.4 Hz, 1H), 8.18 (d, J = 7.4 Hz, 1H), 8.00 (dd, J = 8.6, 1.5 Hz, 1H), 7.66 (dd, J = 17.4, 8.4 Hz, 2H), 7.55 (q, J = 8.6 Hz, 1H), 7.31 (t, J = 7.5 Hz, 1H), 5.49 (s, 1H), 4.51 (t, J = 6.9 Hz, 2H), 3.06 (ddd, J = 16.6, 11.5, 6.4 Hz, 6H), 1.97 (dt, J = 14.6, 7.1 Hz, 2H), 1.76 (ddd, J = 20.9, 10.2, 6.3 Hz, 3H), 1.21 (t, J = 7.3 Hz, 6H). TOF MS: m/z calculated for $C_{21}H_{26}N_2O^+$ M^+: 323.70, found: 323.78.

(E)-2-(2-(9-(4-(diethylamino)butyl)-9H-carbazol-3-yl)vinyl)-3-ethylbenzo[d]thiazol-3-ium ***(CZ-BT)***

To a 50 mL round bottom flask, 2-methyl-3- ethyl benzothiazole iodide (305 mg, 1 mmol) and (E)-2-(2-(9-(4- (diethylamino) butyl) -9H- carbazole -3-yl) vinyl)-3- ethylbenzo [d] thiazol -3-ium (322 mg, 1 mmol) were dissolved in ethanol (15 mL), then several drops of

piperidine was added. The reaction mixture was refluxed for 10 hours under the protection of nitrogen. After cooling down to room temperature, the precipitate was filtered and purified by silica gel column chromatography (dichloromethane: methanol = 18:1, v/v) to afford the brick red powder (146 mg, 24%). ^{1}H NMR (400 MHz, DMSO-d_6) δ 8.98 (s, 1H), 8.46 – 8.37 (m, 1H), 8.33 – 8.18 (m, 1H), 8.03 (d, J = 15.5 Hz, 1H), 7.86 (dd, J = 18.3, 9.0 Hz, 1H), 7.75 (t, J = 7.6 Hz, 1H), 7.56 (t, J = 7.6 Hz, 1H), 7.34 (t, J = 7.4 Hz, 1H), 5.00 (d, J = 7.0 Hz, 1H), 4.53 (s, 1H), 3.07 (d, J = 6.6 Hz, 3H), 1.46 (dd, J = 36.5, 29.4 Hz, 2H), 1.16 (dd, J = 17.8, 10.8 Hz, 4H); ^{13}C NMR (100 MHz, DMSO-d_6) δ 8.98, 8.44, 8.42, 8.40, 8.27, 8.25, 8.24, 8.05, 8.01, 7.89, 7.87, 7.85, 7.82, 7.77, 7.75, 7.58, 7.56, 7.54, 7.36, 7.34, 7.33, 1.52, 1.50, 1.48, 1.17, 1.15, 1.13. TOF HRMS: m/z calculated for $C_{31}H_{36}N_3S^+$ M^+: 482.2620, found: 482.2625.

2.4. UV-vis and fluorescence spectroscopic studies

CZ-BT was dissolved in dimethyl sulfoxide (DMSO) to prepare a concentration of 1.0 mM as the stock solution for further use. The UV-vis and fluorescence spectra were obtained on an Agilent Cary 60 UV−vis spectrophotometer (G6860A) and Agilent Cary Eclipse fluorescence spectrophotometer at room temperature. The absorption and emission spectra were performed by fixed **CZ-BT** concentration (10.0 μM) and titrated with increasing oligonucleotides concentrations using a 1.0 cm length quartz curette. Before recording the spectrum, each oligonucleotide was added into the solution gently, and then stirred and allowed to equilibrate for at least 1.0 min. Each experiment was carried out for three times in replicate determination.

*2.5. The two-photon properties of **CZ-BT** probe*

It is difficult to measure the two-photon fluorescence collection efficiency of molecules directly. Therefore, for comparing the two-photon induced fluorescence of unknown sample and standard sample with known two-photon absorption cross section, the two-photon absorption cross section of target molecule was obtained. The two-photon confocal fluorescence microcopy was used as the test platform, and the sample was tested by infrared pulse laser. In this work, the fluorescein of NaOH aqueous solution (pH=11) was chosen as

reference [29], the two-photon absorption cross section of **CZ-BT** was calculated according to the following formula:

$$\delta_s = \delta_r (S_s \Phi_r \psi_r C_r) / (S_r \Phi_s \psi_s C_s)$$

The subscript of *s* and *r* represented sample and reference; δ was two-photon absorption cross section; *S* indicated the fluorescence signal intensity recorded by charge coupled device (CCD), that was the integral value of fluorescence intensity; Φ expressed the fluorescence quantum yield; ψ showed the fluorescence collection efficiency of experimental device ($\psi_r = \psi_s$), *C* was the concentration of solution. In order to minimize the experimental error, repeated three times for average.

For the double logarithmic plot of two-photon induced fluorescence integral intensity against the average laser power, whether the signal measured was a simple two-photon induced fluorescence could be confirmed. If the slope of the fitting line was close to 2, then the signal was proved as two-photon absorption.

*2.6. The lifetime measurements of **CZ-BT***

The lifetime experiments were carried out by the time-correlated single photon counting (TCSPC) technique (PicoQuant PicoHarp 300) at room temperature. Using deconvolution/fit program (PicoQuant FluFit), the time resolution was reached down to 10 ps. The second harmonic of a titanium sapphire laser (Mai Tai DeepSee) at 400 nm (150 fs, 80 MHz) was selected as excitation source.

*2.7. Molecular modelling study of **CZ-BT** and G4 DNA*

The crystal structure of human telomeric G4 DNA (Telo21, PDB: 4DA3) was used as a receptor to perform docking study on **CZ-BT**. The 3D structures of **CZ-BT** were sketched using chem3D. Autodock Tools (ver. 1.5.6) was used to convert the structure files to pdbqt format. Docking calculation was performed using the AUTODOCK vina program. The dimensions of the active site box were chosen to be large enough to

encompass the entire G4 structures. An exhaustiveness of 100 was used and other parameters were left as default.

2.8. Circular dichroism (CD) spectroscopy test

CD studies were performed on the Chirascan circular dichroism spectrophotometer (Jasco J-810, Japan). The circular dichroism spectra of Telo21 and other DNAs were recorded with and without the addition of **CZ-BT** (20 μM) in Tris-HCl buffer solution (10 mM, 60 mM KCl, pH=7.4) at room temperature using a cuvette with a 1 mm path length over a wavelength range of 220-320 nm with 1 nm bandwidth and the step size of 1 nm. The CD spectra were obtained by taking the average of repeat three times. The final analyses of the data were carried out using Origin 8.0 (Origin Lab Corp).

2.9. Cell digestion and laser confocal imaging

MCF-7 and COS7 cells were cultured in high glucose DMEM supplemented with 10% FBS and penicillin/streptomycin from Gibco in CO_2 incubator at 37°C. The cells were seeded into a confocal glass bottom dish (35.0 mm dish with 20.0 mm bottom well) with 2.0 mL of culture medium in the incubator until the cell density was approximately 50% and then washed with PBS for three times and fixed with ice ethanol. The cell dishes were stored in the refrigerator at minus twenty degree for ten minutes, and washed with PBS for 3 times, DNase and RNase were added into different experimental groups for digestive enzyme and incubated for several hours and then **CZ-BT** (2.0 μM) was added and incubated for 30 min. The fluorescent images were recorded by confocal laser fluorescent scanning microscope under the two-photon excitation wavelength of 820 nm and the emission spectra was recorded within the range of 580-620 nm.

*2.10. The impact of **CZ-BT** on cell cycle*

Plant cells: The cells in exponential phase of growth were digested and transferred into a 6-well flatbottomed plate with the density of 1×10^6 per milliliter; Add drugs:

After 24 hours cultivation, the cell density was reached up to almost 50%. Two milliliters of fresh medium was added into each well of the plate, after removing the original medium out and washed for three times by PBS. Different concentrations of **CZ-BT** and PDS were added and then incubated at 37°C in incubator for another 24 hours. Collect cells: Transferred the original medium into centrifuge tubes, then the cells were digested by pancreatic enzyme and collected into the previous tubes; Fix cells: The cells were collected with centrifugation under the speed of 1500 rpm for 5min, then washed for two times by PBS. Two milliliters of precooled ethanol (70%) was added into the cell suspension under low vortex, then immobilized for 12 hours at 4°C; PI staining: 0.5 ml of PI staining solution was added into every cell sample separately, overhanging cell precipitation slowly and incubated far from light in 37°C for 30 min; Flow cytometer detection: Red fluorescence was detected using an acoustic focusing cytometer, then the effects of **CZ-BT** and PDS on the cell phases were determined on microplate reader spectrophotometer (Thermo Fisher Scientific).

3. Results and discussion

*3.1. Synthesis of **CZ-BT***

Compound **1** was obtained by the reaction of carbazole and 1,4-dibromobutane with the yield of 80%; the ethylated compound **2** was prepared by following the substitution of bromine with diethyl amino in 65% yield; the C-3 aldehyde reaction of **2** with phosphorus oxychloride in dimethyl formamide gave the compound **3** (43%); the condensation reaction of compound **3** and ethylated benzothiazole afforded the desired compound **CZ-BT** (24%, Scheme 1.). **CZ-BT** and its intermediate products were purified by silica gel column chromatography and confirmed by ^{1}H NMR, ^{13}C NMR, and HRMS spectrometry (see the Supplementary Information).

*3.2. The spectra studies of **CZ-BT** upon interaction with G4 DNAs*

The absorbance increased linearly with the increasing concentration of **CZ-BT**

indicating its good solubility in Tris-HCl buffer solution (Fig. S1). **CZ-BT** shows a very low intrinsic fluorescence in Tris-HCl ($\Phi_{F\text{-free}}$=0.01), which is of prime importance for a fluorescent probe for G4 DNA detection. Upon binding with DNAs (ssDNA: dA21, dT21, ss26 and ssDNA; dsDNA: Poly(A-T)$_9$ and Poly(G-C)$_9$; G4 DNA: Telo21, Hum24, Oxy12 and Pu22), the fluorescence intensity of **CZ-BT** was significantly enhanced ($\Phi_{F\text{-DNA}}$ =0.109, Table S1) with the gradual addition of Telo21 with good selectivity (Fig. 1B and Fig. S2). A good linear relationship between fluorescent intensity and the concentration of Telo21 was presented in Figure 1D with the linear correlation coefficient of 0.991 and the detection limit of 15.6 nM.

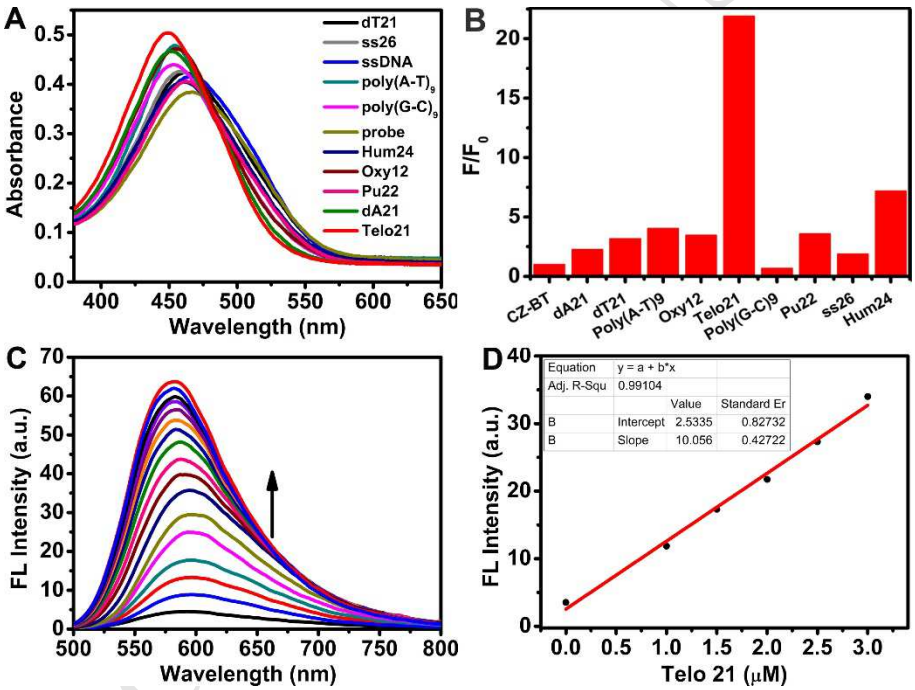

Fig. 1. The absorbance spectra (A) and fluorescence intensity histogram (B) of **CZ-BT** (10.0 μM) in the absence and presence of DNAs in Tris-HCl buffer solution (10 mM, 60 mM KCl, pH=7.4); (C) The fluorescence spectra of **CZ-BT** (10.0 μM) upon titration with Telo21 (0-15.0 μM), λ_{ex}=460 nm; (D) The linear relationship between the fluorescent intensity of **CZ-BT** and the concentrations of Telo21 (0-3.0 μM), n=3.

CZ-BT in Tris-HCl buffer solution presented a freedom state, so there was no rotational restriction around the methine bridge which connect the carbazole and benzothiazole, therefore **CZ-BT** exhibited negligible fluorescence in low viscosity buffer. When the rotation of methine bridge was restrained after binding with G4 DNA

in the high viscosity glycerol solvent, the fluorescence was recovered. This interpretative statement was further supported by the correlation between fluorescence quantum yield and solvent viscosity (Fig. S3) [30].

The two-photon properties of **CZ-BT** was confirmed by a power dependence experiment. Fig. S4A showed the double logarithmic plot of two-photon induced fluorescence integral intensity against the average laser power, a linear regression equation (Log (F_s-$F_{background}$) = 1.95 Log W + 6.07) with a slope of 1.95 was obtained, which indicated an obvious two-photon absorption process. The maximum two-photon absorption cross section of **CZ-BT** was 21.0 GM at the presence of G4 DNA in Tris-HCl buffer solution when excited at 820 nm (Fig. S4B).

*3.3. The impact of G4 DNA on lifetime of **CZ-BT***

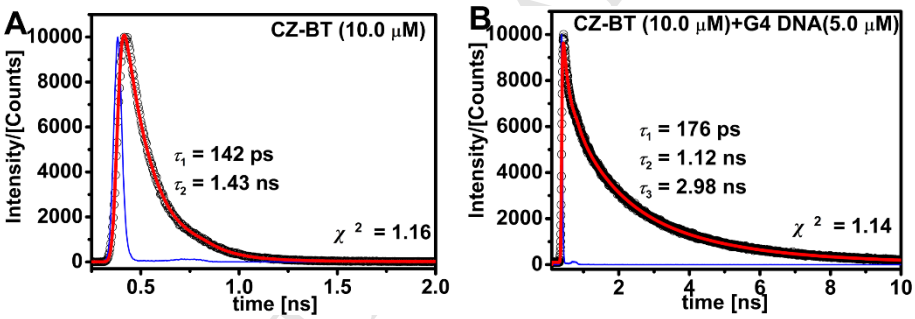

Fig. 2. (A) Lifetimes of **CZ-BT** (10.0 μM) and (B) Lifetimes of **CZ-BT** (10.0 μM) mixed with G4 DNA (5.0 μM) in Tris-HCl buffer solution. The detection wavelength was 580 nm. Fitting results were obtained by a deconvolution of the instrument response function (blue line).

In order to further confirm the interaction between **CZ-BT** and G4 DNA (Telo21), the lifetimes of **CZ-BT** in the absence and presence of G4 DNA were recorded using TCSPC technique excited at 400 nm. Free **CZ-BT** presented a fluorescence lifetime about 1.43 ns and a short lifetime about 142 ps owing to the fast twisting process of C=C double bond between carbazole and benzothiazole (Fig. 2A). As shown in Fig. 2B and Table S2, the proportion of twisting process (τ_1) significantly decreased (from 96.9% to 4.67%) after the interaction with G4 DNA, meanwhile, besides the fluorescence lifetime of free **CZ-BT** (τ_2), there was a new longer lifetime (τ_3) which was assigned to the fluorescence lifetime of **CZ-BT** fixed by G4 DNA [31]. The results above

suggested that the fast twisting process of C=C double bond could be inhibited and the fluorescence lifetime of **CZ-BT** would become longer in the presence of G4 DNA, those are the reasons why the fluorescence intensity of **CZ-BT** increased after the interaction with G4 DNA.

*3.4. Binding mode between **CZ-BT** and G4 DNA*

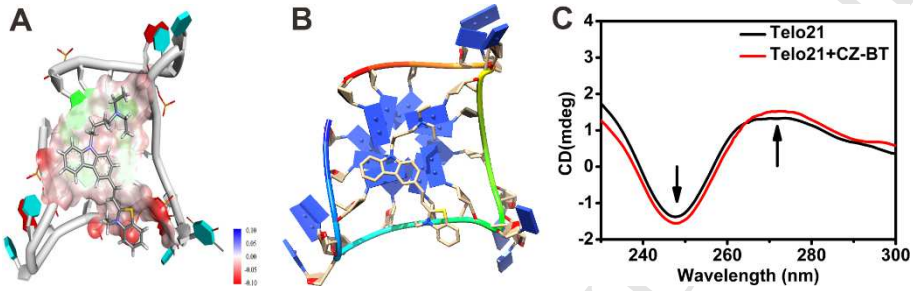

Fig. 3. Top view of the interaction between **CZ-BT** and the charge on Telo21 (PDB id 4DA3) (A) or not (B); (C) Circular dichroism spectrum of Telo21 (20.0 μM) and with the addition of **CZ-BT** (20.0 μM).

The molecular docking study was performed using the AUTODOCK 4.2 program to explore the interaction between **CZ-BT** and G4 DNA. Computation result showed that **CZ-BT** was able to stack onto the Telo21 (PDB id 4DA3) [32] via π-π stacking interaction. Whether there is charge on G4 (Fig. 3A) or not (Fig. 3B), this π-π stacking mainly embodied on the interaction between the aromatic nucleus of **CZ-BT** and purine ring of DG3 in G4. In addition, the secondary structure change of G4 DNA after the interaction with **CZ-BT** was recorded by circular dichroism (CD). As shown in Fig 3C, the CD spectrum of Telo21 structure alone was of the typical antiparallel G4 DNA, with the positive band (272 nm) and negative band (247 nm) [33]. The addition of **CZ-BT** to G4 DNA solution only made the peaks increased, while other DNAs were not changed obviously (Fig. S5). The results indicated that **CZ-BT** did not change the conformation transition of G4 DNA structure. This was also consistent with the fluorescent signal enhancements from the fluorescence titration experiments.

*3.5. Application of **CZ-BT** for the specificity on G4 DNA in cells*

The applications of **CZ-BT** as a selective probe for the detecting and imaging of G4

DNA in cells were further investigated using two-photon confocal laser scanning microscopy. As shown in Fig. 4 (and Fig. S6), **CZ-BT** was able to induce a strong fluorescence response in the regions of nucleus and mainly located in nucleoli where rDNA (ribosomal DNA) undergoes transcription. It has been reported that G-rich rDNA may also adopt temporal quadruplex conformations [34]. The fluorescence signal of **CZ-BT** in nucleus was almost disappeared after DNase treatment, while nothing has changed after RNase treatment in compared with control, which indicated that **CZ-BT** could selectively interact with G4 DNA in cells and generated strong fluorescence.

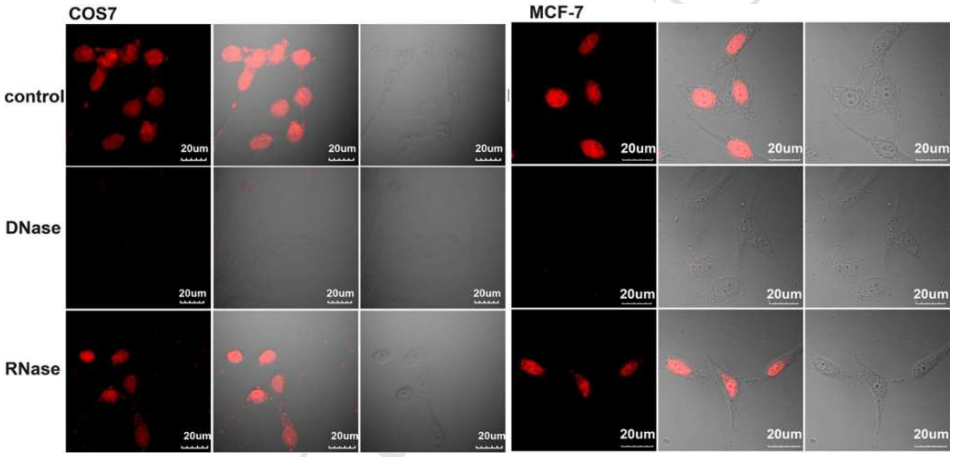

Fig. 4. Digestion experiments for two-photon fluorescence images of fixed COS7 and MCF-7 cells with **CZ-BT** (2.0 μM), λ_{ex}=820 nm, collection wavelength: 600±20 nm, scale bar: 20 μm.

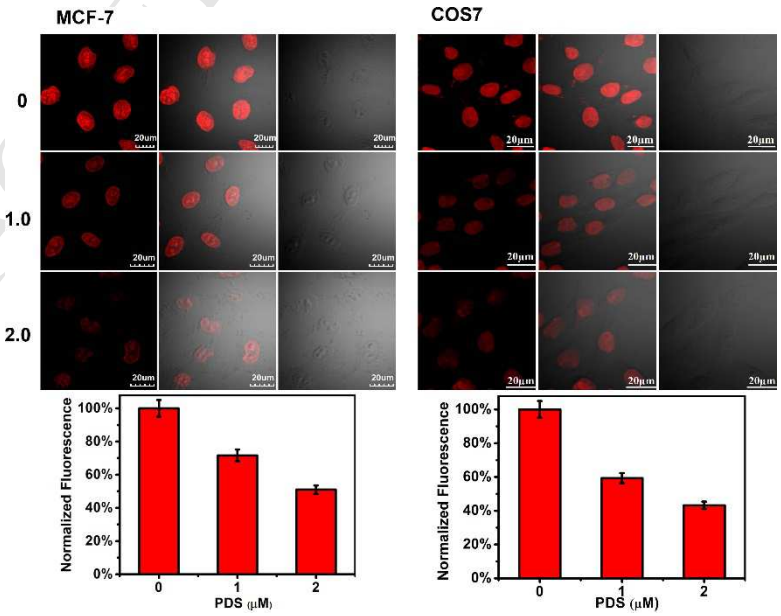

Fig. 5. Two-photon **CZ-BT** (2.0 μM) fluorescence images and the corresponding normalization intensity of fixed MCF-7 and COS7 cells with the addition of PDS (0, 1.0, 2.0 μM). λ_{ex}= 820 nm, collection wavelength: 600±20 nm scale bar: 20 μm.

As a classical G-quadruplex ligand, PDS could promote growth arrest in cells by inducing replication and transcription dependent DNA damage [35]. Therefore, PDS was introduced as the contrast reagent with **CZ-BT** for the endogenous cellular G4 DNA target. As shown in Fig. 5 and Fig. S7, strong fluorescence was presented in the nucleus after the incubation of **CZ-BT**, while the fluorescence intensity was dramatically decreased along with the addition increasing of PDS. This can be attributed to the preferential occupation of G4 DNA binding sites by PDS. Therefore, the specificity of **CZ-BT** on the G4 DNA in cells was verified.

*3.6. The cell cycle experiment of **CZ-BT***

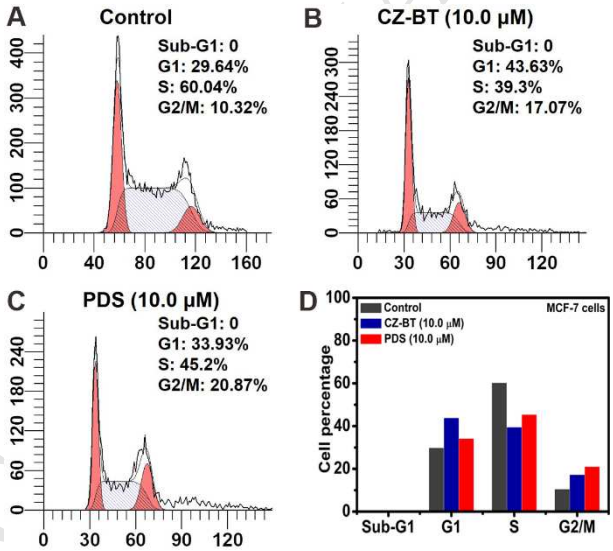

Fig. 6. Effects of **CZ-BT** on cell cycle distribution of MCF-7 cells. The cells were treated with control (A), **CZ-BT** (B), and PDS (C) for 24h, (D) showed the cell cycle percentage distribution. The concentration of **CZ-BT** and PDS was 10.0 μM.

Cell cycle refers to the whole process of a cell from the beginning to the end of the division and each phase preserves different function, respectively [36]. G2 phase is the late period of DNA synthesis, therefore the vast majority of G4 DNAs are accumulated in this phase during the whole cell cycle and the cell growth would be stagnated at G2 stage after the incubated

with PDS [37]. Cells were treated with control, **CZ-BT**, and PDS for 24 h respectively, and then were analyzed by flow cytometry to determine the influence on cell cycle (Fig. 6 and Fig. S8). In comparison with the control group (cells were treated with PBS), the G2 phase population of MCF-7 cells showed a remarkable increasement (10.32% to 17.07%) after the treatment with **CZ-BT** (10.0 μM), which is similar with that of PDS. Therefore, the selective interaction on G4 DNAs of two-photon probe **CZ-BT** with low cytotoxicity (Fig. S9) was fully proved.

4. Conclusion

In conclusion, a novel two-photon fluorescent probe **CZ-BT** of carbazole-benzothiazole derivative for G4 DNA in *vitro* and *vivo* was designed and synthesized. UV-vis, fluorescence emission and lifetime showed the good specificity of **CZ-BT** on G4 DNA, and the molecular docking calculation proved that the binding mode between **CZ-BT** and G4 DNA was π-π stacking. More importantly, the two-photon confocal fluorescent images and cell cycle experiment demonstrated the specificity of **CZ-BT** on G4 DNA in cells. All these results suggested that **CZ-BT** could have promising applications in G4 DNA research.

Conflicts of interest

There are no conflicts of interest to declare.

Acknowledgements

This work was financially supported by the National Natural Science Foundation of China (21421005, 21576037, 21703025 and 21878039) and the NSFC-Liaoning United Fund (U1608222)

References

1 Gellert M, Lipsett MN, Davies DR. Helix formation by guanylic acid. Proc Natl Acad Sci USA 1962;48:2013-2018.

2 Bochman ML, Paeschke K, Zakian VA. DNA secondary structures: stability and function of G-quadruplex structures. Nat Rev Genet 2012;13:770-780.

3 Burge S, Parkinson GN, Hazel P, Todd AK Neidle S. Quadruplex DNA: sequence, topology and structure. Nucleic Acids Res 2006;34:5402-5415.

4 Bidzinska J, Cimino-Reale G, Zaffaroni N, Folini M. G-Quadruplex structures in the human genome as novel therapeutic targets. molecules 2013;18:12368-12395.

5 Dexheimer TS, Sun D, Hurley LH. Deconvoluting the structural and drug-recognition complexity of the G-Quadruplex-forming region upstream of the bcl-2 P1 promoter. J Am Chem Soc 2006;128:5404-5415.

6 Blackburn EH. Structure and function of telomeres. Nature 1991;350:569-573.

7 Biffi G, Tannahill D, McCafferty J, Balasubramanian S. Quantitative visualization of DNA G-quadruplex structures in human cells. Nat Chem 2013;5:182-186.

8 Rhodes D, Lipps HJ. G-quadruplexes and their regulatory roles in biology. Nucleic Acids Res 2015;43:8627-8637.

9 Ou TM, Lu YJ, Tan JH, Huang ZS, Wong KY, Gu LQ. G-quadruplexes: targets in anticancer drug design. Chem Med Chem 2008;3:690-713.

10 Rezler EM, Seenisamy J, Bashyam S, Kim MY, White E, Wilson WD, Hurley LH. Telomestatin and diseleno sapphyrin bind selectively to two different forms of the human telomeric G-quadruplex structure. J Am Chem Soc 2005;127:9439-9447.

11 Chambers VS, Marsico G, Boutell JM, Antonio MD, Smith GP, Balasubramanian S. High-throughput sequencing of DNA G-quadruplex structures in the human genome. Nat Biotechnol 2015;33:877-881.

12 Wu ZS, Chen CR, Shen GL, Yu RQ. Reversible electronic nanoswitch based on DNA G-quadruplex conformation: a platform for single-step, reagentless potassium detection. Biomaterials 2008;29:2689-2696.

13 Ge BX, Huang YC, Sen D, Yu HZ. Arobust electronic switch made of immobilized duplex/quadruplex DNA. Angew Chem Int Ed 2010;49:9965-9967.

14 Zhang J, Chen JH, Chen RC, Chen GN, Fu FF. An electrochemical biosensor for ultratrace terbium based on Tb^{3+} promoted conformational change of human telomeric G-quadruplex. Biosens Bioelectron 2009;25:378-382.

15 Henderson A, Wu YL, Huang YC, Chavez EA, Platt J, Johnson FB, Brosh RM, Sen D, Lansdorp PM. Detection of G-quadruplex DNA in mammalian cells. Nucleic Acids Res 2014;42:860-869.

16 Kim HN, Lee EH, Xu ZC, Kim HE, Lee HS, Lee JH, Yoon J. A pyrene-imidazolium derivative that selectively recognizes G-quadruplex DNA. Biomaterials 2012;33:2282-2288.

17 Yang P, Cian AD, Teulade-Fichou MP, Mergny JL, Monchaud D. Eangineering bisquinolinium/thiazole orange conjugates for fluorescent sensing of G-quadruplex DNA. Angew Chem Int Edit 2009;48:2188-2191.

18 Seo YJ, Lee IJ, Yi JW, Kim BH. Probing the stable G-quadruplex transition using quencher-free end-stacking ethynyl pyrene-adenosine. Chem Commun 2007;27:2817-2819.

19 Vummidi BR, Alzeer J, Luedtke NW. Fluorescent probes for G-quadruplex structures. ChemBioChem 2013;14:540-558.

20 Schnell U, Dijk F, Sjollema KA, Giepmans BNG, Immunolabeling artifacts and the need for live-cell imaging. Nat Methods 2012;9:152-158.

21 Wu SR, Wang LL, Zhang N, Liu Y, Zheng W, Chang A, Wang FY, Li SQ, Shangguan DH. A bis(methylpiperazinylstyryl) phenanthroline as a fluorescent ligand for G-quadruplexes. Chem-Eur J 2016;22:6037-6047.
22 Zuffo M, Ladame S, Doria F, Freccero M. Tuneable coumarin-NDI dyads as G-quadruplex specific light-up probes. Sensor Actuat B-Chem 2017;245:780-788.
23 Wang MQ, Wu Y, Wang ZY, Chen QY, Xiao FY, Jiang YC, Sang A. G-quadruplex DNA fluorescence sensing by a bis-amine-substituted styrylquinolinium dye. Dyes Pigments 2017;145:1-6.
24 Liu Q, Guo BD, Rao ZY, Zhang BH, Gong JR. Strong two-photon-induced fluorescence from photostable, biocompatible nitrogen-doped graphene quantum dots for cellular and deep-tissue imaging. Nano Letters 2013;13:2436-2441.
25 Lim CS, Masanta G, Kim HJ, Han JH, Kim HM, Cho BR. Ratiometric detection of mitochondrial thiols with a two-photon fluorescent probe. J Am Chem Soc 2011;133:11132-11135.
26 Yu HB, Xiao Y, Jin LJ. A lysosome-targetable and two-photon fluorescent probe for monitoring endogenous and exogenous nitric oxide in living cells. J Am Chem Soc 2012;134:17486-17489.
27 Sun W, Cui JX, Ma LL, Lu ZL, Gong B, He L, Wang RB. Analyst 2018;143:5799-5804.
28 Grande V, Shen CA, Deiana M, Dudek M, Olesiak-Banska J, Matczyszyn K, Wurthner F. Chem. Sci 2018;9:8375-8381.
29 Xu C, Webb WW. Measurement of two-photon excitation cross sections of molecular fluorophores with data from 690 to 1050 nm. J Opt Soc Am B 1996;13:481-491.
30 Granzhan A, Ihmels H, Viola G. 9-donor-substituted acridizinium salts: versatile environment-sensitive fluorophores for the detection of biomacromolecules. J Am Chem Soc 2007;129:1254-1267.
31 Byrne CD, Mello AJ. Photophysics of ethidium bromide complexed to ct-DNA: a maximum entropy study. Biophys Chem 1998;70:173-184.
32 Lu YJ, Deng Q, Hou JQ, Hu DP, Wang ZY, Zhang K, Luyt LG, Wong WL, Chow CF. Molecular engineering of thiazole orange dye: change of fluorescent signalling from universal to specific upon binding with nucleic acids in bioassay. ACS Chem Biol 2016;11:1019-1029.
33 Balagurumoorthy P, Brahmachari SK, Mohanty D, Bansal M, Sasisekharan V. Hairpin and parallel quartet structures for telomeric sequences. Nucleic Acids Res 1992;20:4061-4067.
34 Drygin D, Siddiqui-Jain A, O`Brien S, Schwaebe M, Lin A, Bliesath J, Ho CB, Proffitt C, Trent K, Whitten JP, Lim JKC, Hoff DV, Anderes K, Rice WG. Anticancer activity of CX-3543: a direct inhibitor of rRNA biogenesis. Cancer Res 2009;69:7653-7661.
35 Muller S, Kumari S, Rodriguez R, Balasubramanian S. Small-molecule-mediated G-quadruplex isolation from human cells. Nat Chem 2010;2:1095-1098.
36 Sherr CJ. Cancer cell cycles. Science 1996;274:1672-1677.
37 Koirala D, Dhakal S, Ashbridge B, Sannohe Y, Rodriguez R. A single-molecule platform for investigation of interactions between G-quadruplexes and small-molecule ligands. Nat Chem 2011;3:782-787.

Highlights

1: A novel two-photon carbazole based fluorescent probe (**CZ-BT**) was designed and synthesized for specific interaction on G4 DNA with excellent optical properties and large conjugate plane.

2: Compared with ssDNA and dsDNA, **CZ-BT** selectively impacted on G4 DNA with excellent fluorescent emission.

3: Combined with lifetime, molecular docking, circular dichroism, co-staining with PDS (a classical commercial G-quadruplex ligand), nucleic digestion experiments and cell cycle experiments showed **CZ-BT** was specifically impacted on G4 DNA in cells.